



Khan, M. A. H., Brierley, J., Tait, K. N., Bullock, S., Shallcross, D. E., & Lowenberg, M. H. (2022). The Emissions of Water Vapour and NO_x from Modelled Hydrogen-Fuelled Aircraft and the Impact of NO_x Reduction on Climate Compared with Kerosene-Fuelled Aircraft. *Atmosphere*, 13(10), [1660]. <https://doi.org/10.3390/atmos13101660>

Publisher's PDF, also known as Version of record

License (if available):
CC BY

Link to published version (if available):
[10.3390/atmos13101660](https://doi.org/10.3390/atmos13101660)

[Link to publication record in Explore Bristol Research](#)
PDF-document

This is the final published version of the article (version of record). It first appeared online via MDPI at <https://doi.org/10.3390/atmos13101660>. Please refer to any applicable terms of use of the publisher.





University of Bristol - Explore Bristol Research

General rights

This document is made available in accordance with publisher policies. Please cite only the published version using the reference above. Full terms of use are available: <http://www.bristol.ac.uk/red/research-policy/pure/user-guides/ebr-terms/>

Article

The Emissions of Water Vapour and NO_x from Modelled Hydrogen-Fuelled Aircraft and the Impact of NO_x Reduction on Climate Compared with Kerosene-Fuelled Aircraft

M. Anwar H. Khan ^{1,*} , Joel Brierley ², Kieran N. Tait ² , Steve Bullock ² , Dudley E. Shallcross ¹ and Mark H. Lowenberg ^{2,*} 

¹ Atmospheric Chemistry Research Group, School of Chemistry, Cantock's Close, University of Bristol, Bristol BS8 1TS, UK

² Department of Aerospace Engineering, University of Bristol, Queens Building, University Walk, Bristol BS8 1TR, UK

* Correspondence: anwar.khan@bristol.ac.uk (M.A.H.K.); m.lowenberg@bristol.ac.uk (M.H.L.)

Abstract: A kerosene fuelled aircraft was modelled within a performance tool and fuel burn and the emissions of nitrogen oxides (NO_x) and water vapour at different stages of flight throughout the mission were estimated. Adaptions were made to engine and aircraft parameters within the performance tool to accommodate a liquid hydrogen fuel over the same given mission. Once an iterative design process had been completed to ensure the aircraft could perform the given mission, the performance tool was again used to calculate total fuel burn. Fuel burn results alongside predicted emission indices were used to estimate the emissions of NO_x, water vapour from hydrogen-fuelled aircraft. The use of hydrogen fuel over kerosene fuel in the modelled aircraft resulted in the removal of carbon-based emission species alongside 86% reduction in NO_x and 4.3 times increase in water vapour emission. The climate impact of this switch with the reduction in NO_x emission was assessed by a 3D global atmospheric chemistry and transport model, STOCHEM-CRI, which found a significant reduction in the concentration of a potent greenhouse gas, ozone, and an oxidizing agent, OH, by up to 6% and 25%, respectively. The reduction of OH levels could induce a positive radiative forcing effect as the lifetime of another important greenhouse gas, methane, is increased. However, the magnitude of this increase is very small (~0.3%), thus the overall impact of the reduction in NO_x emissions is likely to have a net negative radiative forcing effect, improving aviation's impact on the environment. However, further work is warranted on effects of other emission species, specifically water vapour, particulate matter and unburned hydrogen.

Keywords: liquid hydrogen; kerosene fuel; greenhouse gas; radiative forcing; aviation industry



Citation: Khan, M.A.H.; Brierley, J.; Tait, K.N.; Bullock, S.; Shallcross, D.E.; Lowenberg, M.H. The Emissions of Water Vapour and NO_x from Modelled Hydrogen-Fuelled Aircraft and the Impact of NO_x Reduction on Climate Compared with Kerosene-Fuelled Aircraft. *Atmosphere* **2022**, *13*, 1660. <https://doi.org/10.3390/atmos13101660>

Academic Editor: Yongming Han

Received: 30 August 2022

Accepted: 10 October 2022

Published: 12 October 2022

Publisher's Note: MDPI stays neutral with regard to jurisdictional claims in published maps and institutional affiliations.



Copyright: © 2022 by the authors. Licensee MDPI, Basel, Switzerland. This article is an open access article distributed under the terms and conditions of the Creative Commons Attribution (CC BY) license (<https://creativecommons.org/licenses/by/4.0/>).

1. Introduction

Over recent years, the world has experienced a sharp increase in greenhouse gas emissions (e.g., CO₂) through industrialisation and globalisation which has in turn had a negative impact on climate change (e.g., global warming). The anthropogenic emissions of CO₂ have increased at a rate of 5% y⁻¹ for 2013 to 2018 which has risen from 2.2% y⁻¹ over the period 1970 to 2012 [1]. If unnatural global warming trends enhanced by this scenario continue along the same trajectory in the future, increased droughts in tropical regions could devastate food crops, while the loss of ice in polar regions could result in a significant sea-level rise creating millions of environmental refugees [2]. One of the transport sectors, aviation, has grown strongly over time and globally it contributes ~1.9% of greenhouse gas emissions, ~2.4% of CO₂ emissions and ~3.5% of effective radiative forcing [1]. Thus, one of the efforts that needs to be made to decrease greenhouse gas emissions is from the aviation sector. This is further shown by aircraft manufacturers looking to develop aircraft

that operate on alternative fuels (e.g., biofuels, hydrogen, ammonia, electric, nuclear) rather than fossil fuel.

In aircraft, currently kerosene, a hydrocarbon fuel, is burned and a variety of chemical species such as CO₂, CO, NO_x, SO_x, and other particulates (e.g., soot) are emitted [3,4]. The life cycle of kerosene has many negative environmental impacts [5]. Even before it is burned in an engine, the extraction, refinement, and transport of the fuel from ground sources of crude oil contributes to hydrocarbon emissions which can be oxidized to ultimately form CO₂. This process can be prone to adverse events such as oil spills, further increasing its potential negative impact on the environment. Once the kerosene has been refined from crude oil, it is transported again before being burned, resulting in increased emissions in the atmosphere. Compared with the initial process of extraction, refinery and transportation, the burning of kerosene produces greater amounts of CO₂, e.g., kerosene carbon intensity for the EU-27 region is 93.1 gCO₂eq/M with extraction of 10 gCO₂eq/M, refining of 6.1 gCO₂eq/M, transportation of 3 gCO₂eq/M and burning of 74 gCO₂eq/M [6], therefore has the greatest impact on the greenhouse effect. The largest positive warming effects, come from CO₂ and non-CO₂ terms (e.g., contrail cirrus and NO_x driven changes) in the atmosphere [1]. Comparing the forcing of CO₂ and non-CO₂ terms, to halt aviation's growing contribution to global warming, it is necessary to achieve net-zero CO₂ emissions as well as decreasing non-CO₂ radiative forcing. For this reason, finding alternative fuels for the aviation industry is important with the aim of decarbonisation of emissions due to CO₂ providing the greatest contribution to greenhouse gases.

Liquid hydrogen is one of the possible alternatives to kerosene fuel for use in aviation. Airbus is looking to develop hybrid-hydrogen aircraft, powered by the combustion of a liquid hydrogen fuel [7]. Many studies [8,9] showed the potential uses of hydrogen as a fuel for aviation, due to its advantages in terms of energy content and environmental pollution. Hydrogen has an energy density per unit mass approximately 2.9 times greater than that of kerosene [10] but energy density per unit volume is much greater for kerosene, thus the space that hydrogen would occupy would be around 4 times larger than that of kerosene [11]. Hydrogen fuel shares multiple positive characteristics with current fuels, such as being storable and transportable which is essential for aviation—although liquid hydrogen needs to be kept at a temperature less than −253 °C and the volume requirements make it unsuitable for storage in the wings. The main disadvantages highlighted include the requirement for large and potentially heavy, pressurized tanks that do not experience boil-off due to molecular size of hydrogen, increased drag and weight due to larger wetted area to accommodate the higher fuel volume, greater complexity in systems for pumping fuel from the cryogenic tanks to engines, difficulty in achieving rapid and safe refuelling as well as potential cost of production [12].

When burnt, liquid hydrogen only produces H₂O and small amounts of NO_x as waste products [13]. Production of NO_x is related to the flame temperature within the engine and hydrogen-air flames can be of greater temperature than kerosene-air flames under the same conditions [14]. However, Agarwal et al. [15] showed that hydrogen combustion could potentially produce up to 90% less NO_x than kerosene fuel. As the emission of NO_x is directly linked to the production of ozone, kerosene operated aircraft NO_x emissions can contribute up to 3 ppbv to upper tropospheric background ozone levels [16]. The tropospheric ozone is one of the leading contributors to anthropogenic radiative forcing from aviation, thus the change of NO_x emissions due to the switch of kerosene to hydrogen fuel and its impact on the radiative forcing is an important area of investigation.

Hydrogen combustion would produce approximately 2.6 times more water vapour than an equivalent mass of kerosene [17,18]. In theory, hydrogen combustion should not produce particulate matter (PM). However, aircraft's lubrication system and oil could emit a nonnegligible amount of PM [19,20], but the overall PM emissions from hydrogen aircraft compared with kerosene aircraft will be small. Due to the reduction of PM emission from hydrogen-fuelled aircraft, the formation of condensation trails would potentially decrease resulting in the reduced radiative forcing effect of contrails [17]. Thus, the emissions from

hydrogen fuel and their complete combustion products (e.g., H_2O , NO_x) could have less impact on climate. However, it is important to investigate the accumulated radiative forcing effects of the emissions of hydrogen-based flight to kerosene-based flight.

In this study, we calculate the emission produced by a model aircraft, an approximation to an Airbus A320, operating with kerosene fuel compared with an equivalent liquid hydrogen fuelled aircraft over a 3000 nautical mile (nmi) mission; the effect of the changes in emissions on climate due to the shift of kerosene flights to hydrogen flights are then investigated by a global 3D atmospheric chemistry and transport model, STOCHEM-CRI.

2. Methods

For investigating the fuel burn and emissions from an aircraft operating with liquid hydrogen fuel compared with a kerosene equivalent, a performance model is deployed for two aircraft with comparable design objectives. The performance model implements a standard iterative mission performance analysis using the Breguet range equation, the details of this model can be found in Brierley [21]. For assessing the potential benefits of replacing current aircraft with hydrogen fuelled alternatives, it is assumed that they would have to meet the same operational demands. To ensure meaningful comparison, the hydrogen-fuelled aircraft is designed to carry the same payload mass over the same range as the existing conventionally fuelled aircraft selected for the study, i.e., the Airbus A320 which can carry approximately 160 passengers over a range of 3000 nmi [21]. This is done using a Breguet range-based performance tool to identify values such as block fuel burn and block time of the mission. Values obtained from the performance code can then be used alongside a range of methods to calculate emissions produced by the kerosene aircraft throughout the mission. Following on from this, aircraft and engine parameters are adjusted to accommodate a hydrogen fuel system before the performance analysis code is used again to recalculate fuel burn for the hydrogen aircraft and estimate the emissions produced.

To accommodate changes in the fuel system, adaptations in both volume and weight of the aircraft relative to the kerosene-fueled version were required due to increased mass and volume of the hydrogen fuel tanks. This involved an increase in both length and cross-sectional area of the fuselage and affected both profile and induced drag acting on the aircraft; the mass and volume effects were accounted for using the scale factors derived by Verstraete [11] and the drag coefficient changes were estimated using a preliminary aircraft design method from [22]. Further mass penalties from [11] were also considered due to the requirement of additional structural components to support increased aircraft mass. An iterative design process was then undertaken using the performance tool to size the aircraft, taking into account all aspects previously stated, to ensure the aircraft was able to perform the required mission whilst carrying a suitable amount of reserve fuel [21]. From here, mass of hydrogen fuel burned throughout the mission are calculated.

2.1. Emission Calculation

The emissions of two species, water vapour and NO_x , are considered for comparing the modelled hydrogen fuelled aircraft with a kerosene fuelled aircraft. The quantities of unburned fuel, hydrocarbons and PM emitted were assumed negligible and were not considered in the calculation. There is a lack of literature and pre-established methods for calculating the emissions from hydrogen fuelled aircraft, thus we used the methods based on the comparison of emission indices (EIs) and total emissions of both the kerosene and hydrogen aircraft in question. The EIs for the kerosene aircraft are calculated by a combination of the Boeing Fuel Flow Method 2 (BFFM2), International Civil Aviation Organisation (ICAO) engine databank values for the CFM56-5B engine and the Fuel Composition Method which have been briefly described in Wasiuk et al. [23].

When hydrogen is burned as an aviation fuel, it produces approximately 2.55 times more water vapour than from an equivalent mass of kerosene [17,18]. This is shown by comparing the EIs of each fuel that are quoted relative to the energy content of fuel burned,

reflected here in terms of mass of kerosene required to produce that energy level. The EIs for hydrogen and kerosene are 3.21 kg(H₂O)/kg(kerosene) and 1.26 kg(H₂O)/kg(kerosene), respectively [17]. The energy density of kerosene is 42.8 MJ/kg [24] meaning these EIs show that hydrogen and kerosene emit 3.21 kg and 1.26 kg of H₂O, respectively per 42.8 MJ of fuel burned. For this study, it was necessary to establish an EI representing the relationship between mass of H₂O emitted and mass of hydrogen burned. As the relationship between the fuel EIs is based on energy content of fuel burned, the EI for hydrogen was multiplied by the ratio of the fuels' energy densities to obtain an EI relative to mass of hydrogen burned (hydrogen has an energy density of 122.8 MJ/kg [24]). As the energy density of the hydrogen fuel is 2.87 times greater than that of kerosene, the EI was multiplied by this ratio to predict an EI of 9.21 kg(H₂O)/kg(H₂). This EI is then multiplied by the total mass fuel burn calculated by the performance tool to give a total amount of water vapour emitted.

Comparison of different combustion systems has shown predictions of ~80–90% reduction in NO_x emissions relative to a kerosene fuelled aircraft when using a micromix combustor [14,15,25]. Therefore, to predict NO_x emissions, EIs for the kerosene reference aircraft were reduced by 80%. It was still assumed that NO_x production would be affected by fuel flow rate and atmospheric conditions so EIs for each mode of the mission were used as they were for the kerosene aircraft. Once reduced, EIs for cruise and the modes of the landing and take-off (LTO) cycle are used to calculate total NO_x emitted.

2.2. Atmospheric Modelling

To assess the change in climate impact due to the switch from kerosene to hydrogen fuelled aircraft, a 3D global chemistry and transport model, STOCHEM-CRI was used. This model was originally developed by the UK Meteorological Office but subsequently the component of the model accounting for chemical processes has been updated. STOCHEM-CRI utilises a 3 h time step for the advection of its 50,000 constant mass air parcels that represent the Earth's troposphere [26]. It is within these isolated air parcels that the chemical reactions and photochemical dissociations leading to the loss and production of trace gases are considered to be taking place. This archived meteorological data (pressure, temperatures, winds, clouds, humidities, tropopause heights, precipitation, boundary layer depth and surface parameters) is itself from the UKMO Hadley Centre global general circulation model called the Unified Model (UM) and means that the model is able to run offline [27]. A Lagrangian approach for advection allows uncoupling of the chemistry and transport processes and these cells are based on a grid resolution of 1.25° longitude, 0.833° latitude and 12 unevenly spaced (with respect to altitude) vertical levels between the surface and an upper boundary of ~100 mbar [26]. The description of the meteorological parameterisations (e.g., vertical coordinate, advection scheme, boundary layer treatment, inter-parcel exchange and convective mixing) can be found in Cooke [28].

The chemical mechanism used in STOCHEM is the common representative intermediates version 2 and reduction 5 (CRI v2-R5) which was built using a series of five-day box model simulations on each compound, on a compound-by-compound basis. Developed initially by Jenkin et al. [29] with subsequent improvement by Watson et al. [30], Utembe et al. [31,32], and Jenkin et al. [33], the CRI scheme involves the most reduced mechanism, making it suitable for global modelling due to its traceability. Contained within STOCHEM-CRI is a full description of tropospheric photochemistry, free radical reactions and physical removal processes (dry and wet deposition) that process emissions of major tropospheric trace gases.

The base case (referred to as STOCHEM-base) involves the STOCHEM-CRI run with the aircraft NO_x emissions (4.1 Tg/y) from a 4D Aircraft Fuel Burn and Emissions Inventory [34] for the year 2011. To estimate the effects of reduced NO_x emissions due to a switch from kerosene fuel to hydrogen fuel in the aircraft, two simulations (referred to as STOCHEM-50NO_x, STOCHEM-75NO_x) were performed with 50% and 75% aircraft NO_x reductions relative to a base case of standard aircraft emissions. The output from these

two simulations (STOCHEM-50NO_x, STOCHEM-75NO_x) and comparing them with the STOCHEM-base simulation will show the impact of reduced NO_x emissions on climate.

3. Results and Discussion

3.1. Performance Analysis

The performance analysis of the modelled kerosene and hydrogen Airbus A320-like aircraft carrying the same payload over the 3000 nmi mission generates a payload-range diagram as shown in Figure 1. This shows that both variants achieve the 3000 nmi design range with the specified payload and that this is lower than the maximum payload for the aircraft (i.e., the amount of fuel required to fly 3000 nmi means that the maximum take-off weight is reached at a lower payload than maximum available payload capacity: adding any further payload would make the take-off mass exceed the maximum allowable). Furthermore, the kerosene-fuelled variant has a greater range when carrying maximum payload (2267 nmi, point A_{kerosene} in the figure) when compared with the hydrogen alternative (1855 nmi, point A_{hydrogen}); and the hydrogen aircraft has a lower zero payload range, or 'ferry range', of 3336 nmi when compared with a ferry range of 3748 nmi for the kerosene model—points B_{kerosene} and B_{hydrogen}. This occurs due to the higher zero-fuel mass of this aircraft and the lower mass density of the hydrogen fuel, causing aircraft mass to decrease less as fuel is burnt during the mission, thus impacting maximum range.

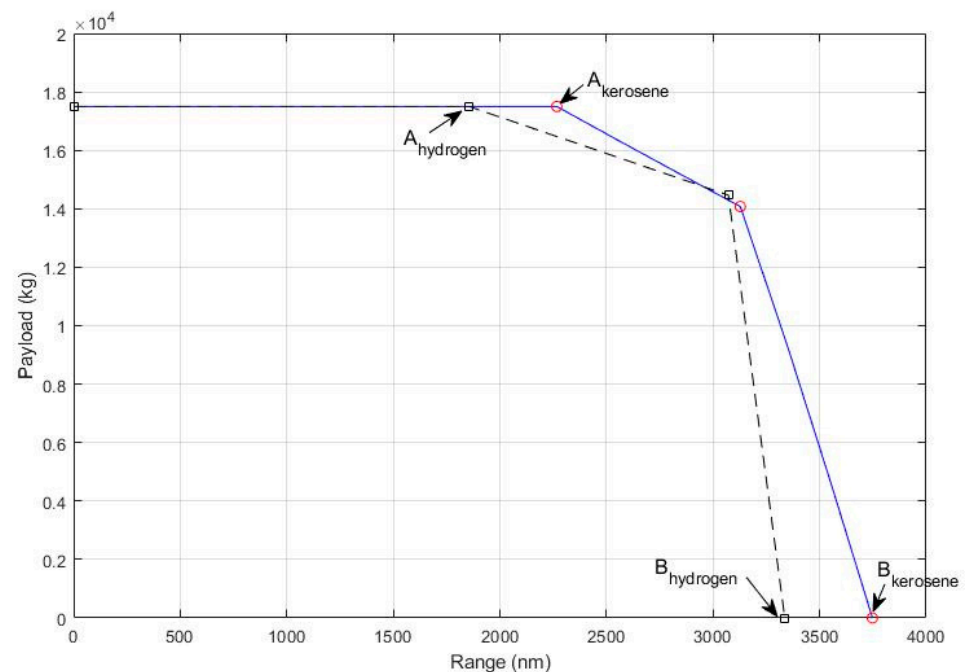


Figure 1. Payload range diagram for kerosene (solid line) and hydrogen fuelled (dashed line) aircraft.

The performance tool is used to calculate the required fuel burn for the chosen mission of carrying 160 passengers over 3000 nmi for each fuel. The calculated fuel burns were found to be 13,999 kg of kerosene and 8141 kg of hydrogen, showing a 41% reduction in mass of fuel burned. This decrease in fuel burn was expected due to the difference in energy densities. The energy density with respect to mass of hydrogen is about 2.87 greater than that of kerosene [24] causing the reduced fuel mass burned. However, the ratio of the fuel burns is not of this magnitude. Increased mass and drag of the hydrogen fuelled aircraft means that the mass of fuel burned in the hydrogen aircraft only decreased by a factor of 1.72 relative to the kerosene alternative.

3.2. Emissions

Assuming no CO₂, CO, unburned hydrogen, hydrocarbon and PM emissions from hydrogen fuelled aircraft, we only show the comparison of the emissions of water vapour

(H₂O) and NO_x for both modelled flights (see Table 1). Note that in this study the cruise is at constant altitude (32,000 ft) and the term LTO refers here to everything except the cruise (taxi, take-off, climb; descent, landing, taxi).

Table 1. Predicted H₂O and NO_x emissions from model kerosene-fuelled and hydrogen-fuelled aircraft.

Kerosene Fuel Aircraft			
Species	Cruise Emissions (kg)	LTO Cycle Emissions (kg)	Total Emissions (kg)
H ₂ O	14,890	2522	17,412
NO _x	222.1	5.9	228.0
Hydrogen fuel aircraft			
H ₂ O	58,640	16,360	75,000
NO _x	23.7	7.2	30.9

The predicted emission of H₂O (75,000 kg) from the hydrogen fuelled aircraft is found to be 4.31 times greater than the kerosene fuelled aircraft emission (17,412 kg). Initially, the EIs show hydrogen to produce 2.55 times more water vapour than an equivalent mass of kerosene with equivalent energy content [17,18]. Similarly to the fuel burn calculation, a greater energy content of hydrogen is burned due to increased mass and drag therefore further increasing H₂O emissions from the hydrogen fuelled aircraft. This result demonstrates the concern of greatly increased amounts of water vapour, and thus contrails, that could stem from using hydrogen as an aviation fuel.

The NO_x emission from hydrogen fuelled aircraft is found to be one order of magnitude lower (23.7 kg) than kerosene fuelled aircraft (222.1 kg) during the cruise phase of flight. However, the emissions within the LTO cycle, during take-off and climb, is found to be slightly higher (7.2 kg) in hydrogen fuelled aircraft compared with kerosene fuelled aircraft (5.9 kg), although they are only maintained for a short period of time, especially compared with time in cruise. Overall, the total NO_x emissions are reduced in hydrogen fuelled aircraft by 86% compared with kerosene fuelled aircraft which agrees with existing literature, reinforcing the idea of liquid hydrogen being a fuel that has the potential to greatly improve aviation's impact on the atmosphere. This is just a prediction and would greatly benefit from the ability to test a hydrogen powered engine to obtain emission data like that of the ICAO databank used for kerosene engines. This would also show the quantity of unburned fuel emitted that is not accounted for in this study.

3.3. Climate Impact

The STOCHEM-50NO_x and STOCHEM-75NO_x runs simulate the reduced NO_x emissions due to the use of hydrogen fuelled aircraft over kerosene fuelled aircraft and their impacts on chemistry and transport of the atmospheric composition. The comparison of these simulations with the STOCHEM-base simulation shows how the reduction of NO_x affects the distribution and magnitude of global NO_x and the major constituent atmospheric trace species concentrations (e.g., ozone, OH, CH₄) which have the potential to influence global climate change.

The reduced NO_x emissions in STOCHEM-75NO_x and STOCHEM-50NO_x compared with STOCHEM-base have a significant effect at 7.2–16.2 km (404–100 hPa) where the global NO_x mixing ratios are reduced between 0° N and 90° N with a maximum reduction of 40% and 25%, respectively in 30° N to 55° N at the top of the troposphere (11.8–16.2 km; 201–100 hPa) (see Figure 2). The impact on the southern hemisphere (SH) is also visible where the decrease in NO_x mixing ratios at 11.8–16.2 km (201–100 hPa) is found in STOCHEM-75NO_x and STOCHEM-50NO_x to be 15% and 10%, respectively.

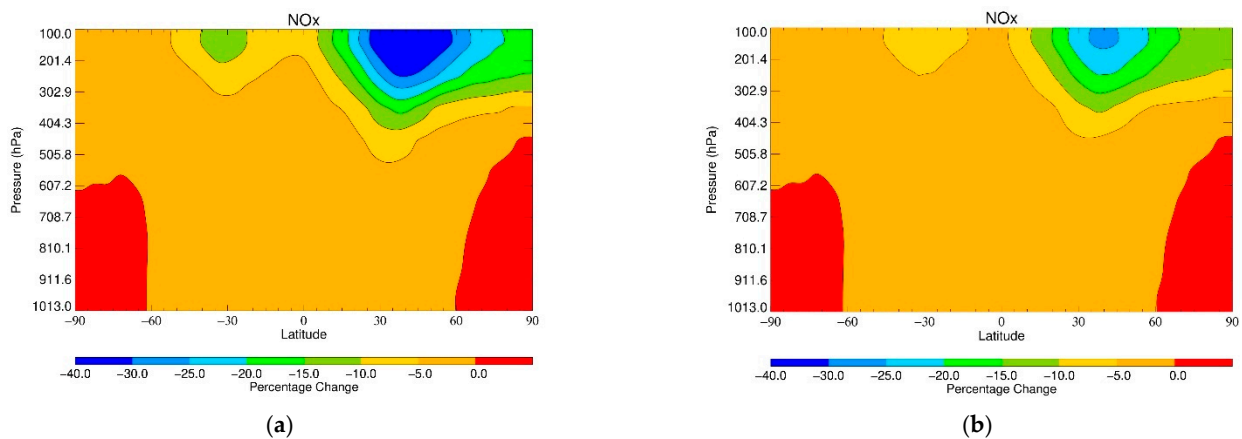


Figure 2. The percentage zonal change of NO_x mixing ratios from (a) STOCHEM-base to STOCHEM-75 NO_x scenario, (b) STOCHEM-base to STOCHEM-50 NO_x scenario. Note: The approximate height equivalent to the pressure in the y -axis can be found in Appendix A (Table A1).

The longitude-latitude distribution plots (Figure 3) show that the percent decrease of NO_x mixing ratios is biggest at 11.8–16.2 km (201–100 hPa) where it is confined mainly to the 10° – 90° N latitude band. There are pronounced decreases of NO_x by 60% (in STOCHEM-75 NO_x) and 30% (in STOCHEM-50 NO_x) over eastern North America, mainland Europe and the transatlantic corridor (Figure 3). A decrease of 20% (in STOCHEM-75 NO_x) and 15% (in STOCHEM-50 NO_x) is also visible in the SH in eastern Australia extending to the French Polynesia in the South Pacific Ocean and eastern Brazil (Figure 3).

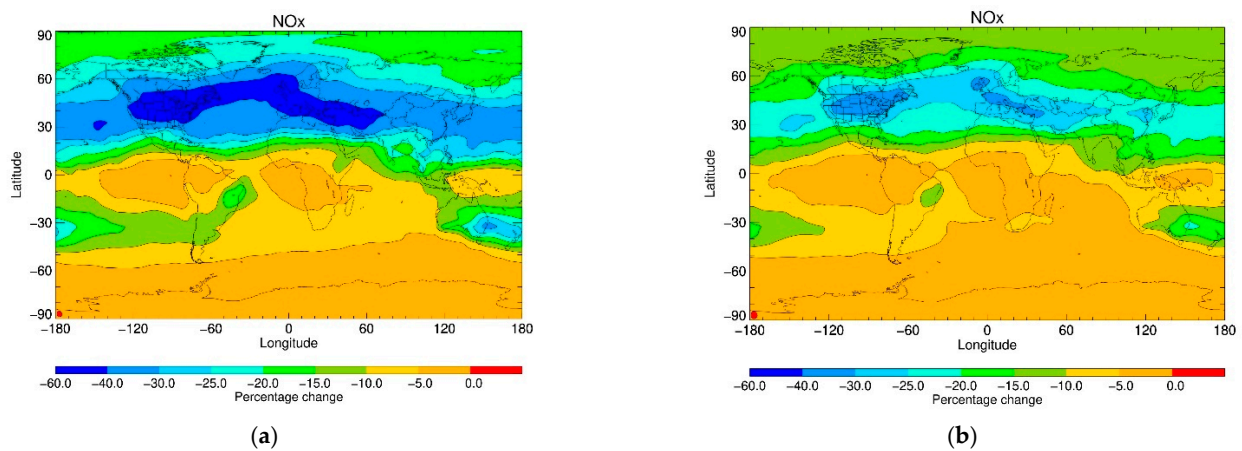


Figure 3. The percentage surface change of NO_x mixing ratios at 11.8–16.2 km (201–100 hPa) from (a) STOCHEM-base to STOCHEM-75 NO_x scenario, (b) STOCHEM-base to STOCHEM-50 NO_x scenario.

The reduced emissions of NO_x in STOCHEM-75 NO_x and STOCHEM-50 NO_x decreases the global mixing ratios of ozone exclusively in the NH, most notably above 7.2 km, with maximum decreases of 6% and 3.5%, respectively at 11.8–16.2 km (201–100 hPa) in 40° – 50° N (Figure 4). The reduction in NO emissions from hydrogen aircraft causes a reduced production of NO_2 from the reaction of $\text{NO} + \text{HO}_2/\text{RO}_2$, resulting in the reduced photolysis of NO_2 which reduces the production of ozone. This decrease in ozone would decrease radiative forcing, therefore working to improve aviation's impact on the environment.

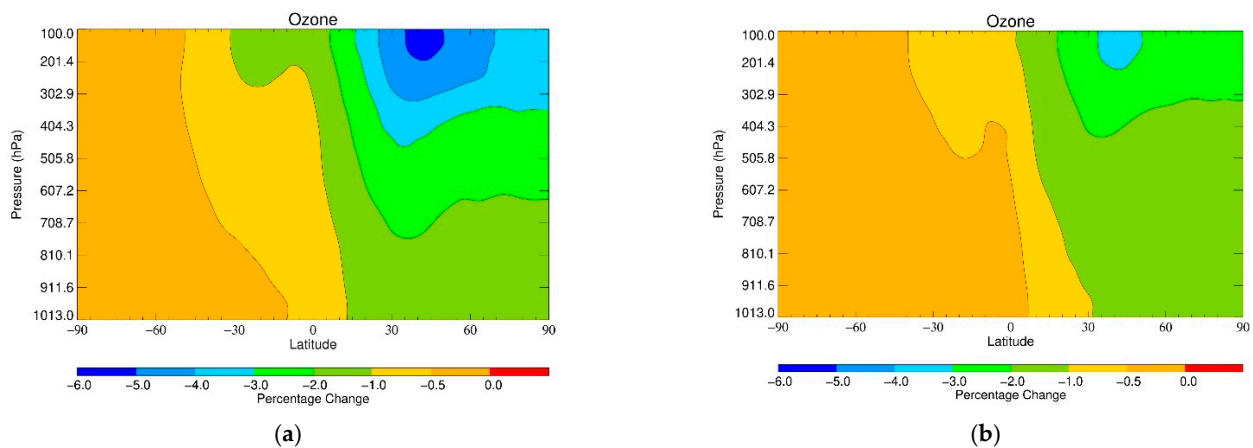


Figure 4. The percentage zonal change of ozone mixing ratio from (a) STOCHEM-base to STOCHEM-75NO_x scenario, (b) STOCHEM-base to STOCHEM-50NO_x scenario. Note: The approximate height equivalent to the pressure in the *y*-axis can be found in Appendix A (Table A1).

The distribution plot of surface ozone mixing ratios change from STOCHEM-base to STOCHEM-75NO_x shows a maximum decrease in ozone mixing ratios of ~6% at 11.8–16.2 km (201–100 hPa) starting from 20° N to 50° N over eastern North America, mainland Europe and the transatlantic corridor (Figure 5). The trend is mirrored on a slightly smaller scale (reduced by 4%) in the case of the change of ozone mixing ratios from STOCHEM-base to STOCHEM-50NO_x.

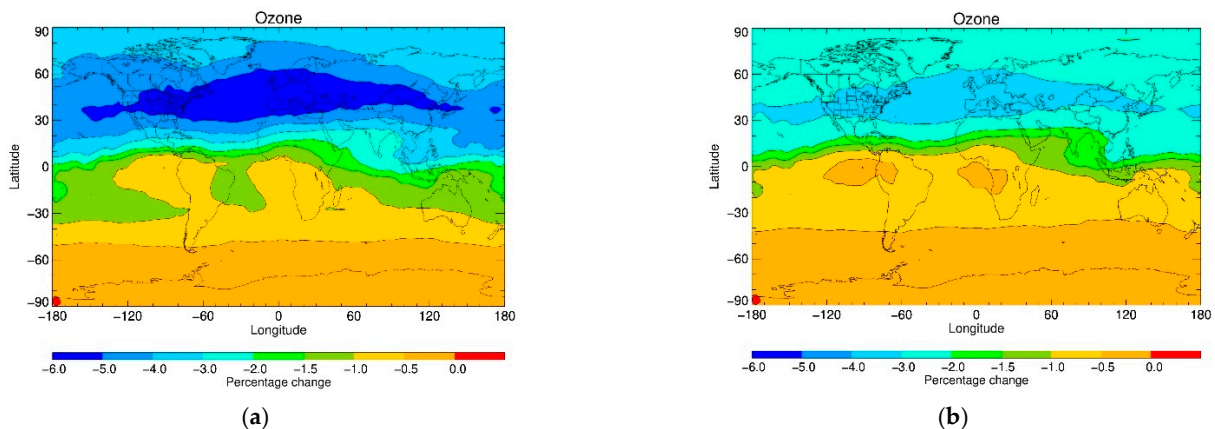


Figure 5. The percentage change of ozone mixing ratios at 11.8–16.2 km (201–100 hPa) from (a) STOCHEM-base to STOCHEM-75NO_x scenario, (b) STOCHEM-base to STOCHEM-50NO_x scenario.

Reduced NO_x mixing ratios are shown to greatly reduce quantities of OH present in the atmosphere. The reductions of up to 25% and 15% over parts of the northern hemisphere are found from 7.2 to 16.2 km (404 to 100 hPa) during a transition from STOCHEM-base to STOCHEM-75NO_x and STOCHEM-base to STOCHEM-50NO_x, respectively. The photolysis of ozone forms extremely reactive excited atomic oxygen, (O(¹D))), which can react with water and produces most of the tropospheric OH. As the abundances of ozone decreases (Figures 4 and 5), the production of OH also decreases resulting in decreased OH mixing ratios (Figure 6).

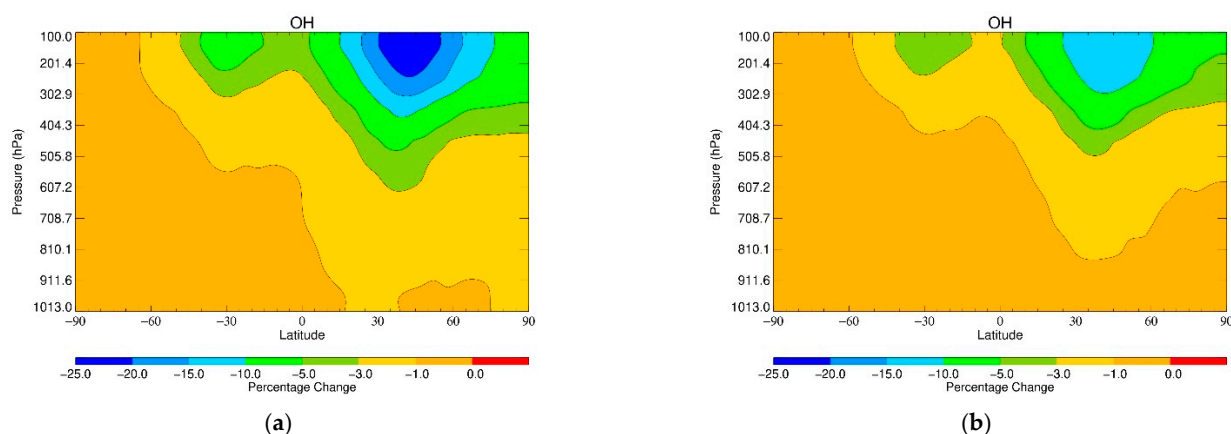


Figure 6. The percentage zonal change of OH from (a) STOCHEM-base to STOCHEM-75NO_x scenario and (b) STOCHEM-base to STOCHEM-50NO_x scenario. Note: The approximate height equivalent to the pressure in the y-axis can be found in Appendix A (Table A1).

This is important as OH radical quantities relate to the lifetime of other greenhouse gases present in the atmosphere. Reduction in OH inhibits the oxidation reactions and thus increases the quantity of hydrocarbon species such as methane remaining in the atmosphere. Therefore, decreasing OH levels could induce a positive radiative forcing effect as the lifetime of species such as methane could be increased.

Figure 7 shows the increase in CH₄ mixing ratios induced by the reduced NO_x, but the magnitude of this increase is very small (0.2 to 0.3%) in comparison to the changes in ozone experienced (4 to 6%). Considering the radiative forcing of methane (0.48 Wm⁻²) and ozone (0.34 Wm⁻²) [35], a back-of-the-envelope calculation shows the net radiative forcing change for the decrease of ozone and increase of methane is ~−0.016 Wm⁻². Therefore, the reduction in NO_x emissions due to the switch from kerosene fuelled aircraft to hydrogen fuelled aircraft is likely to have a net negative radiative forcing effect, improving aviation’s impact on the environment. All the effects discussed are shown to have the greatest effect over the northern hemisphere, in particular Europe and America. This is due to the greater volume of air traffic in these regions inducing the greatest changes.

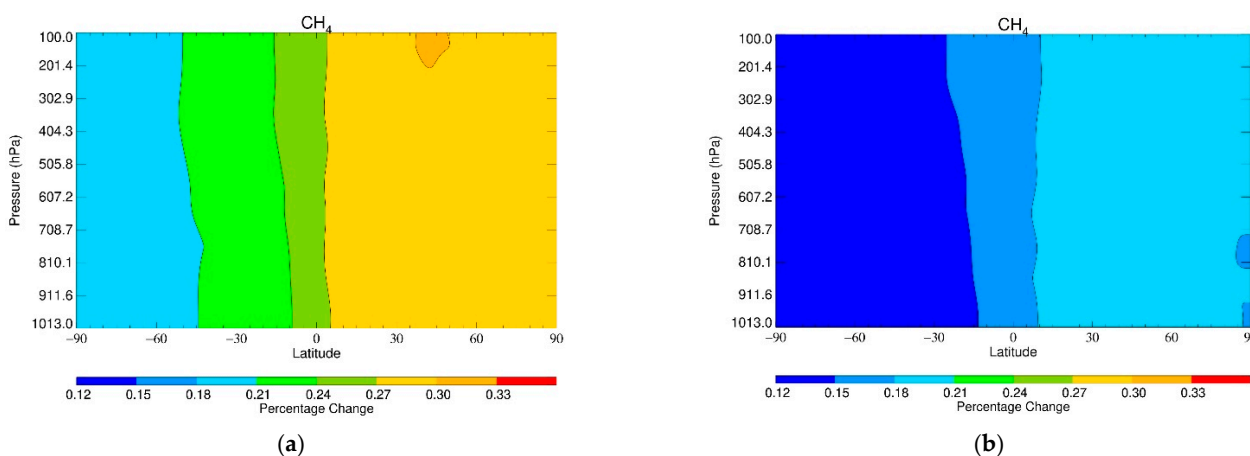


Figure 7. The percentage zonal change of CH₄ mixing ratios from (a) STOCHEM-base to STOCHEM-75NO_x scenario and (b) STOCHEM-base to STOCHEM-50NO_x scenario. Note: The approximate height equivalent to the pressure in the y-axis can be found in Appendix A (Table A1).

One of the main areas of uncertainty in this study is from the design of a hydrogen fuelled aircraft. A more detailed design process would result in increased accuracy of the aircraft modelled in the performance tool. This would result in a more accurate mission fuel burn, causing an increased accuracy in quantities of emissions calculated from this result.

Increased accuracy and confidence in results could lead on to further development in the work on climate impact. Data regarding performance of hydrogen fuelled aircraft would also be developed through analysis of different aircraft models over different missions. In this study one mission profile was assessed and then that comparison was applied to all aircraft present in the flight inventory used for STOCHEM-CRI model runs. Emission change data would be more accurate if a variety of aircraft and missions were to be analysed to estimate trends in net emissions change. The estimated NO_x emission reduction of 86% may have a significant uncertainty as this has not been experimentally validated yet. Experimental measurements are warranted to investigate whether this theoretical reduction in NO_x due to the micromix combustor used is realistic, or whether it is overestimating the potential climate benefit.

In terms of the climate impact study, only the impact of NO_x reduction was studied but there are other factors to consider. Firstly, the use of hydrogen would prevent emissions of CO_2 into the atmosphere, with significant climate benefits which need to be accounted for. Secondly, the effect of the increased water vapour needs to be evaluated, especially the potential changes in contrail formation. This is an important point due to the uncertainty around contrail formation from the increased water vapour emissions of the hydrogen fuel [1]. Despite increased quantities of water vapour, there are negligible amounts of PM arising from aircraft's lubrication system and oil in the emissions to act as nuclei for the water to crystalize around. This means contrails formed from hydrogen exhaust could be "optically thinner" than those formed from kerosene [36], impacting their radiative forcing effect. Finally, the effects of unburned hydrogen were not considered. Emissions of unburned hydrogen could further impact concentration of species such as OH radicals in the atmosphere and therefore needs to be considered in the total impact of burning hydrogen fuel.

4. Conclusions

Using a Breguet range-based aircraft performance tool, a kerosene fuelled aircraft modelled from the original A320 was analysed over a 3000 nmi mission. A variety of methods were used alongside results from the performance tool to calculate the total fuel burn and the emissions of different species from the aircraft. Following this, adaptations were made to engine and aircraft parameters within the performance tool to accommodate the use of liquid hydrogen fuel on the modelled aircraft. Analysis was completed for the hydrogen fuelled aircraft and fuel burn results were used alongside predicted emission indices to estimate NO_x and water vapor emissions from hydrogen fuel. This allowed a comparison of emission species produced by the two fuels in question and led on to comparing the impact on climate from the burning of the two different fuels. This was done by considering the impact of reduced NO_x emissions from aviation on atmospheric composition using a 3D global chemistry and transport model, STOCHEM-CRI.

The emission estimation for using the modelled hydrogen fuelled aircraft over kerosene fuelled aircraft showed an 86% reduction in nitrogen oxides (NO_x) and 4.3 times increase in water vapour emission. The climate impact modelling results concluded that 75% reduced NO_x emissions from hydrogen-fuelled aircraft would likely have a net negative radiative forcing impact (i.e., decrease of ozone concentration by up to 6%), which would be beneficial regarding aviation's impact on the environment. Together with the elimination of carbon emissions, this suggests significant climate benefits from use of liquid hydrogen fuel. Sources of error are high in these results as methods for predicting NO_x and water vapour emissions from hydrogen fuel burn are much less developed than those for kerosene and no detailed design has been completed for the liquid hydrogen fuelled A320-like aircraft considered in this study. A new aircraft design would need to be employed to sustain liquid hydrogen fuels which would be costly, with the production and commercial use of these fleets taking a significant amount of time [13]. However, with the assumptions made in the literature, the study shows that the use of liquid hydrogen fuel over kerosene fuel can be beneficial from an environmental point of view. While switching from kerosene-

to hydrogen-fuelled aircraft could be a viable long-term solution for reducing radiative forcing, it would not enable the aviation industry to reduce CO₂ and NO_x emissions imminently. This is because of the production cost of newly designed aircraft and the manufacturing, storage and transportation issues of green hydrogen fuel. By this time this technology would be ready for commercial use, substantial damage to the climate could already have occurred.

Author Contributions: M.A.H.K. and J.B. investigated the data and wrote the paper; M.H.L., D.E.S. and M.A.H.K. conceived and designed the project; D.E.S., M.H.L., S.B. and K.N.T. reviewed and edited the manuscript. All authors have read and agreed to the published version of the manuscript.

Funding: M.A.H.K. and D.E.S. thank N.E.R.C. grant (A Scientist just like me) (grant reference-2021/EDIE011Shallcross), Bristol ChemLabS and the Primary Science Teaching Trust under whose auspices various aspects of this work was supported. © 2022 all rights reserved.

Institutional Review Board Statement: Not Applicable.

Informed Consent Statement: Not Applicable.

Data Availability Statement: The data presented in this study are available on request from corresponding author.

Conflicts of Interest: The authors declare no conflict of interest.

Appendix A

Table A1. Mean pressures and equivalent height for model output levels [26].

Model Output Level	Mean Pressure (hPa)	Approximate Height (km)
1	1013–912	0.0–1.0
2	912–810	1.0–2.0
3	810–709	2.0–3.0
4	709–607	3.0–4.2
5	607–505	4.2–5.6
6	505–404	5.6–7.2
7	404–302	7.2–9.2
8	302–201	9.2–11.8
9	201–100	11.8–16.2

References

- Lee, D.S.; Fahey, D.W.; Skowron, A.; Allen, M.R.; Burkhardt, U.; Chen, Q.; Doherty, S.J.; Freeman, S.; Forster, P.M.; Fuglestedt, J.; et al. The contribution of global aviation to anthropogenic climate forcing for 2000 to 2018. *Atmos. Environ.* **2021**, *244*, 117834. [CrossRef]
- Butler, C.D. Climate change, health and existential risks to civilization: A comprehensive review (1989–2013). *Int. J. Environ. Res. Public Health* **2018**, *15*, 2266. [CrossRef]
- Tait, K.N.; Khan, M.A.H.; Bullock, S.; Lowenberg, M.H.; Shallcross, D.E. Aircraft emissions, their plume-scale effects and the spatio-temporal sensitivity of the atmospheric response: A review. *Aerospace* **2022**, *9*, 355. [CrossRef]
- Masiol, M.; Harrison, R.M. Aircraft engine exhaust emissions and other airport-related contributions to ambient air pollution: A review. *Atmos. Environ.* **2014**, *95*, 409–455.
- Koroneos, C.; Dompros, A.; Roumbas, G.; Moussiopoulos, N. Life cycle assessment of kerosene used in aviation. *Int. J. LCA* **2005**, *10*, 417–424. [CrossRef]
- Chiaromonti, D.; Talluri, G.; Vourliotakis, G.; Testa, L.; Prussi, M.; Scarlat, N. Can lower carbon aviation fuels (LCAF) really complement sustainable aviation fuel (SAF) towards EU aviation decarbonization? *Energies* **2021**, *14*, 6430. [CrossRef]
- Airbus. How Blue Condor Will Accelerate Airbus First Hydrogen-Powered Test Flights. Available online: <https://www.airbus.com/en/newsroom/stories/2022-07-how-blue-condor-will-accelerate-airbus-first-hydrogen-powered-test-flights> (accessed on 31 August 2022).
- Veziroğlu, T.N.; Barbir, F. Hydrogen: The wonder fuel. *Int. J. Hydrog. Energy* **1992**, *17*, 391–404. [CrossRef]

9. Rosen, M.A.; Koohi-Fayegh, S. The prospects for hydrogen as an energy carrier: An overview of hydrogen energy and hydrogen energy systems. *Energ. Ecol. Environ.* **2016**, *1*, 10–29. [[CrossRef](#)]
10. Najjar, Y. Hydrogen safety: The road toward green technology. *Int. J. Hydrogen Energy* **2013**, *38*, 10716–10728. [[CrossRef](#)]
11. Verstraete, D. The Potential of Liquid Hydrogen for Long Range Aircraft Propulsion. Ph.D. Thesis, Cranfield University, Cranfield, UK, 2009.
12. Tashie-Lewis, B.C.; Nnabuife, S.G. Hydrogen production, distribution, storage and power conversion in a hydrogen economy-A technology review. *Chem. Eng. J. Adv.* **2021**, *8*, 100172. [[CrossRef](#)]
13. Nojoumi, H.; Dincer, I.; Naterer, G.F. Greenhouse gas emissions assessment of hydrogen and kerosene-fueled aircraft propulsion. *Int. J. Hydrog. Energy* **2009**, *34*, 1363–1369. [[CrossRef](#)]
14. Svensson, F. Potential of Reducing the Environmental Impact of Civil Subsonic Aviation by Using Liquid Hydrogen. Ph.D. Thesis, Cranfield University, Cranfield, UK, 2005.
15. Agarwal, P.; Sun, X.; Gauthier, P.; Sethi, V. Injector design space exploration for an ultra-low NO_x hydrogen micromix combustion system GT2019-90833. In Proceedings of the ASME Turbo Expo 2019: Turbomachinery Technical Conference and Exposition, Phoenix, AZ, USA, 17–21 June 2019.
16. Kentarchos, A.S.; Roelofs, G.J. Impact of aircraft NO_x emissions on tropospheric ozone calculated with a chemistry-general circulation model: Sensitivity to higher hydrocarbon chemistry. *J. Geophys. Res.* **2002**, *107*, ACH 8-1–ACH 8-12.
17. Ponater, M.; Pechtl, S.; Sausen, R.; Schumann, U.; Huttig, G. Potential of the cryplane technology to reduce aircraft climate impact: A state-of-the-art assessment. *Atmos. Environ.* **2006**, *40*, 6928–6944. [[CrossRef](#)]
18. Gauss, M.; Isaken, I.S.A.; Wong, S.; Wang, W.C. Impact of H₂O emissions from cryoplanes and kerosene aircraft on the Atmosphere. *J. Geophys. Res. Atmos.* **2003**, *108*, 4304. [[CrossRef](#)]
19. Yu, Z.; Liscinsky, D.S.; Winstead, E.L.; True, B.S.; Timko, M.T.; Bhargava, A.; Herndon, S.C.; Anderson, B.E. Characterization of lubrication oil emissions from aircraft engines. *Environ. Sci. Technol.* **2010**, *44*, 9530–9534. [[CrossRef](#)]
20. Fushimi, A.; Saitoh, K.; Fujitani, Y.; Takegawa, N. Identification of jet lubrication oil as a major component of aircraft exhaust nanoparticles. *Atmos. Chem. Phys.* **2019**, *19*, 6389–6399. [[CrossRef](#)]
21. Brierley, J. Comparison of Emissions from Kerosene and Liquid Hydrogen Fuelled Aircraft and Their Impact on Atmospheric Chemistry. Master's Thesis, University of Bristol, Bristol, UK, 2022.
22. Jenkinson, L.R.; Simpkin, P.; Rhodes, D. *Civil Jet Aircraft Design*; Butterworth-Heinemann: Oxford, UK, 1999; 432p.
23. Wasiuk, D.K.; Lowenberg, M.H.; Shallcross, D.E. An aircraft performance model implementation for the estimation of global and regional commercial aviation fuel burn and emissions. *Transp. Res. Part D Transp. Environ.* **2015**, *35*, 142–159. [[CrossRef](#)]
24. Seeckt, K.; Scholz, D. Jet versus Prop, Hydrogen versus Kerosene for a Regional Freighter Aircraft. Available online: <http://fe.ProfScholz.de> (accessed on 31 August 2022).
25. Funke, H.H.-W.; Keinz, J.; Hendrick, P. Experimental evaluation of the pollutant and noise emissions of the GTCP 36-300 gas turbine operated with kerosene and a low NO_x micromix hydrogen combustor. In Proceedings of the 7th European Conference for Aeronautics and Space Science (EUCASS), Milan, Italy, 3–6 July 2017.
26. Collins, W.J.; Stevenson, D.S.; Johnson, C.E.; Derwent, R.G. Tropospheric ozone in a global-scale three-dimensional Lagrangian model and Its response to NO_x emission controls. *J. Atmos. Chem.* **1997**, *26*, 223–274. [[CrossRef](#)]
27. Cullen, M.J. The unified forecast/climate model. *Meteorol. Mag.* **1993**, *122*, 81–94.
28. Cooke, M.C. Global Modelling of Atmospheric Trace Gases Using the CRI Mechanism. Ph.D. Thesis, University of Bristol, Bristol, UK, 2010.
29. Jenkin, M.E.; Watson, L.A.; Utembe, S.R.; Shallcross, D.E. A Common Representative Intermediates (CRI) mechanism for VOC degradation. Part 1: Gas phase mechanism development. *Atmos. Environ.* **2008**, *42*, 7185–7195. [[CrossRef](#)]
30. Watson, L.A.; Shallcross, D.E.; Utembe, S.R.; Jenkin, M.E. A Common Representative Intermediates (CRI) mechanism for VOC degradation. Part 2: Gas phase mechanism reduction. *Atmos. Environ.* **2008**, *42*, 7196–7204. [[CrossRef](#)]
31. Utembe, S.R.; Watson, L.A.; Shallcross, D.E.; Jenkin, M.E. A Common Representative Intermediates (CRI) mechanism for VOC degradation. Part 3: Development of a secondary organic aerosol module. *Atmos. Environ.* **2009**, *43*, 1982–1990. [[CrossRef](#)]
32. Utembe, S.R.; Cooke, M.C.; Archibald, A.T.; Jenkin, M.E.; Derwent, R.G.; Shallcross, D.E. Using a reduced common representative (CRI v2-R5) mechanism to simulate tropospheric ozone in a 3-D Lagrangian chemistry transport model. *Atmos. Environ.* **2010**, *44*, 1609–1622. [[CrossRef](#)]
33. Jenkin, M.E.; Khan, M.A.H.; Shallcross, D.E.; Bergström, R.; Simpson, D.; Murphy, K.L.C.; Rickard, A.R. The CRI v2.2. reduced degradation scheme for isoprene. *Atmos. Environ.* **2019**, *212*, 172–182. [[CrossRef](#)]
34. Wasiuk, D.K.; Khan, M.A.H.; Shallcross, D.E.; Lowenberg, M.H. A commercial aircraft fuel burn and emissions inventory for 2005–2011. *Atmosphere* **2016**, *7*, 78. [[CrossRef](#)]
35. Forster, P.; Ramaswamy, V.; Artaxo, P.; Berntsen, T.; Betts, R.; Fahey, D.W.; Haywood, J.; Lean, J.; Lowe, D.C.; Myhre, G.; et al. Changes in Atmospheric Constituents and in Radiative Forcing. In *Climate Change 2007: The Physical Science Basis. Contribution of Working Group I to the Fourth Assessment Report of the Intergovernmental Panel on Climate Change*; Solomon, S., Qin, D., Manning, M., Chen, Z., Marquis, M., Averyt, K.B., Tignor, M., Miller, H.L., Eds.; Cambridge University Press: Cambridge, UK; New York, NY, USA, 2007.
36. Schumann, U. Formation, properties and climate effects of contrails. *Comptes Rendus Phys.* **2005**, *6*, 549–565. [[CrossRef](#)]